








Research article

# Use of modified deep eutectic solvent as an additional chemical in a flexible conductive natural rubber sensor for motion analysis

Boripat Sripornsawat<sup>1,2</sup>, Antonia Georgopoulou<sup>2,3</sup>, Sarttawut Tulaphol<sup>1</sup>,  
Anoma Thitithammawong<sup>4</sup>, Jobish Johns<sup>5</sup>, Yeampon Nakaramontri<sup>1\*</sup>, Frank Clemens<sup>2</sup>

<sup>1</sup>Sustainable Polymer & Innovative Composite Materials Research Group, Department of Chemistry, Faculty of Science, King Mongkut's University of Technology Thonburi, Bangkok, Thailand

<sup>2</sup>Department of Functional Materials, Empa-Swiss Federal Laboratories for Materials Science and Technology, Überlandstrasse 129, 8600 Dübendorf, Switzerland

<sup>3</sup>Department of Mechanical Engineering (MECH), Vrije Universiteit Brussel (VUB), and Flanders Make Pleinlaan 2, B-1050 Brussels, Belgium

<sup>4</sup>Department of Rubber Technology and Polymer Science, Faculty of Science and Technology, Prince of Songkla University, Pattani Campus, Pattani, Thailand

<sup>5</sup>Department of Physics, Rajarajeswari College of Engineering, Bangalore, India

Received 13 June 2022; accepted in revised form 22 August 2022

**Abstract.** The strain sensors based on conductive natural rubber (NR) composite, filled with carbon nanotubes (CNT) and conductive carbon black (CCB), are developed due to their superior elasticity and sensitivity. To encourage electron tunneling, ionic pathway for electron moving was achieved by modified deep eutectic solvent (mDES) synthesized in-house. It was found that the incorporation of mDES impacts the curing, mechanical and electrical properties of the composites due to the interconnected CNT/CCB-mDES networks. It is demonstrated that the electrical signal sensation of conductive NR composite was improved by adding mDES, and the inconsistent sensor behavior under cyclic and quasi-static loadings was eliminated. The mDES not only improves the movement of electrons, but it also promotes the crosslinking of NR molecules without adding ZnO. In addition, for analyzing the object motion, the piezoresistive rubber sensors were tested on a soft printing structure through the cyclic motion analysis of a soft tendon-based actuator. The obtained electrical signals showed the smooth signal with noise and un-prediction electrical peaks after the combination of the mDES into the conductive NR composites. This clarifies the flexible movement of the CNT/CCB structure into the NR matrix following the specific designed objects' motion. The present work indicates the different core novel technologies based on the use of mDES in the conductive composites matching with the acceptable electrical signal for applying as the promising motion sensor materials for soft structures.

**Keywords:** rubber, polymer composites, material testing, mechanical properties

## 1. Introduction

Resistive sensors typically convert mechanical, thermal, or chemical stimuli into an electrical signal and are generally fabricated from various materials, selective from metallic to semiconductors and inorganics

to organics [1]. In recent years, the demand for flexible and stretchable strain sensors based on polymer matrix has received enormous attention in wearable electronics, soft robotics, and stretchable devices due to the potential of expressing flexibility, processability,

\*Corresponding author, e-mail: [yeampon.nak@kmutt.ac.th](mailto:yeampon.nak@kmutt.ac.th)  
© BME-PT

and lightweight [1]. Several research groups have succeeded in fabricating stretchable strain sensors by using various forms of thermoplastic elastomer (TPE), *i.e.*, thermoplastic polyurethane (TPU) [2–5], thermoplastic styrene co-block polymers (TPS) [6, 7] and styrenic block copolymers (SBC) [8, 9]. However, it was found that the use of TPE is difficult in highly dynamic strain sensors since the material requires a superior capacity for original shape recovery. It is known that the TPE has both elastic and plastic deformation behaviors. In particular, at high strain monitoring over 20% of extension ratio, plastic deformation occurs. Therefore, it is a new challenge for the development of elastomeric sensors by incorporating synthetic and natural rubbers. Two different hypotheses for using rubber sensors are (i) the lowest hardness of crosslinked rubber [10, 11] and (ii) appropriate elastic properties for reasonable shape recovering time are needed [12]. According to our previous work, we found that the use of pure natural rubber (NR) for applying as the sensor monitor is needed to be developed. With the superior elasticity of NR and its lower plastic deformation during applied stress in comparison to TPE, the cumulative stress originated during stretching and caused strong deformation inside the rubber structure. As a result, the incorporation of hard filler particles into the NR matrix is considered; in particular, the conductive filler helps the NR composites respond to the electrical signals. Among the reinforcing fillers, conductive carbon black (CCB), carbon nanotubes (CNT), and graphene (GP) deliver excellent electrical performances based on their  $sp^2$  hybridized carbon structure pathway of the filler network in the NR matrix [13]. The geometry and morphology of the conductive fillers inevitably influence the formation of conductive networks [14, 15]. Carbon nanoparticles have a strong tendency to agglomerate, which results in high percolation threshold concentration, poor electrical conductivity, and poor electron tunneling across the gaps between adjacent nano-carbon particles in NR composites [16]. Hence, the hybrid filler concept by the combination of CCB and CNT to improve electrical conductivity has been explored [17, 18]. Furthermore, CCB also improves the sensitivity to stress and strain due to its spherical shape that eases the disconnection of conductive particles by strain, while the long cylindrical CNT particles have sliding contact [19, 20]. However, mechanical deformation often results in additional peaks of sensor

signal upon releasing the load and strain [20, 21]. With these drawbacks, using NR in sensor applications is still limited and promising. Finding eco-friendly and cost-effective materials with sensitivity has been proposed, and there are no prior reports available in the literature.

To overcome this problem, the conductive liquid phase inside the NR matrix might organize the transfer of an electron from end-to-end of the filler particles since the liquid will be wetted on filler surface and serves as a better electron bridge between the conductive filler particles [22–24]. Based on the context of green chemistry, the ionic liquid was synthesized by deep eutectic solvent (DES) with free cationic and anionic movements as reported by Azizi *et al.* [25], where DES is a mixture of hydrogen bond donor (HBD, *i.e.* urea, carboxylic acid and polyalcohol) and hydrogen bond acceptor (HBA, *i.e.* choline chloride and quaternary ammonium salt). The preparation of DES in a pure state is simple and economically viable as it shows a 100% atom economy with no need for post-synthesis purification like other ionic liquids. In this case, choline chloride (ChCl) and urea are both naturally biocompatible chemicals that are not hazardous if they are released back into nature separately. The incorporation of DES and modified DES (mDES) into NR and epoxidized NR (ENR) affects vulcanization and mechanical properties and enhances the conductivity of NR and ENR by the formation of intermolecular attraction between rubber molecules [26]. However, DES and mDES in combination with NR composites filled with CNT and CCB, have not been investigated so far. Therefore, it is a new system for the investigation of NR-based sensors.

In the present article, the fabrication of conductive NR composites using CNT-CCB as conductive hybrid filler is reported. To improve the dispersion and conductivity, mDES was prepared by dissolving active ZnO in DES with various DES loadings and added to the conductive NR composite (CNRC). The nature of dispersion was assessed from Payne effect and morphological studies. The chemical crosslinking, mechanical properties, and electrical conductivity of the composites were investigated in detail. Piezoresistivity of the CNRC (strain sensitivity of electrical resistance) was investigated in terms of relative change in resistance,  $\Delta R/R_0$  ( $\Delta R$  and  $R_0$  are the change in resistance with and without the strain of the composite) [27, 28]. Also, both dynamic and

quasi-static deformations were investigated by cyclic tensile testing methods. Finally, the performance of the resulting NR-based sensor was investigated on tendon-based 3D printed actuators to confirm its use in the field of soft robotics. It has to be noted that the uses of DES for improving the sensitivity of the conductive composites are a challenge and promising; the pairing among ChCl and urea was first chosen to modify with the ZnO and apply to the CNRC for studying and examining the sensitivity of the hyper-elastic material.

## 2. Experimental

### 2.1. Materials

For the fabrication of conductive rubber with hybrid filler and ionic liquid concept, natural rubber (NR) was mixed with multi-walled carbon nanotubes (CNT), conductive carbon black (CCB), and modified deep eutectic solvent (mDES). All chemicals used in this study are listed in Table 1, along with their functions and suppliers.

### 2.2. Preparation of modified deep eutectic solvents (mDES)

The mDES was synthesized using ChCl (hydrogen bond acceptor) and urea (hydrogen bond donor) at the molar ratio ChCl: urea of 1:2 [27]. ChCl and urea were mixed at 80 °C for 6 h or until the formation of a homogeneous transparent liquid called DES. Then, active zinc oxide (aZnO) was added in DES at four different weight ratios, namely 1:0.5, 1:1, 1:2 and

1:4 (aZnO:DES) at 80 °C for 24 h. The resulting mDES samples were kept in a desiccator to avoid moisture absorption. The detailed synthesis of DES and mDES has been described elsewhere [26].

### 2.3. Fabrication of NR composites

The NR/CNT-CCB composites with and without mDES were prepared using an internal mixer (model MX75; Charoen tut Co., Ltd., Samutprakarn, Thailand) at a mixing temperature of 80 °C, a rotor speed of 60 rpm, and 75% fill factor of the chamber volume. The mixing process was started by masticating NR in an internal mixer for 1 min at 80 °C and an additional mixing of 5 min after adding the CNT-CCB hybrid nanofillers. Then, the stearic acid and ZnO were incorporated stepwise for min and later mDES for 2 min. Finally, the accelerator and sulfur were consecutively added to the conductive NR compound with continued mixing until reaching 13 min. As a reference, the pure NR and NR/CNT-CCB without mDES were prepared following the same procedure. All compounds were rapidly passed through the 1 mm nip of the two-roll mill continuously 5 times (1 min/time) under the controlled rolling speed of 60 rpm to achieve homogeneous dispersion of CNT-CCB in the NR matrix before conditioning at room temperature in a desiccator for at least 24 h. NR composite sheets with 2 mm thickness were fabricated by using compression molding at 160 °C with the cure times based on rheometer tests. It is noted that the composites with CNT-CCB without and with

**Table 1.** List of chemicals used in the preparation of NR composites with and without mDES along with their functions and suppliers.

Materials	Functions	Suppliers
Natural rubber (Standard Thai Rubber, STR 5L)	Matrix	Nabon Rubber Co., Ltd., Nakorn Si Thammarat, Thailand
Stearic acid	Co-activator in sulfur curing systems	Imperial Chemical Co., Ltd., Pathumthani, Thailand
Active zinc oxide (aZnO)	Modifying agent of DES and activator in sulfur curing systems	Global Chemical Co., Ltd., Samutprakarn, Thailand
Multi-walled carbon nanotubes (CNT; NC7000)	Cylindrical conductive reinforcing filler in rubber	Nanocyl S. A. Sambreville, Belgium
Conductive carbon black (CCB; Vulcan XC72)	Spherical conductive reinforcing filler in rubber	Cabot China Ltd., Shanghai, China
2,2'-Dithiobis-(benzothiazole) (MBTS)	Accelerator in sulfur curing systems	Flexsys Inc., Termoli, Italy
Sulfur	Curing agent	Ajax Chemical Co. Ltd., Samutprakarn, Thailand
Choline chloride (ChCl)	Reactant of DES	Loba Chemie Pvt. Ltd., Maharashtra, India
Urea	Reactant of DES	Elago Enterprises Pty. Ltd., Cherrybrook, Australia

**Table 2.** Composition of all conductive pure NR and NR composites.

Ingredients	Contents [phr]					
	Pure NR	NR-C/mDES <sub>x</sub>				
		0.0	2.5	5.0	10.0	20.0
NR	100.0	100.0	100.0	100.0	100.0	100.0
Stearic acid	1.0	1.0	1.0	1.0	1.0	1.0
aZnO	5.0	5.0	–	–	–	–
CNT-CCB*	–	5.0/7.5	5.0/7.5	5.0/7.5	5.0/7.5	5.0/7.5
MBTS	1.0	1.0	1.0	1.0	1.0	1.0
Sulfur	2.5	2.5	2.5	2.5	2.5	2.5
mDES			7.5	10.0	15.0	25.0
(aZnO:DES)	–	–	(1:0.5)	(1:1.0)	(1:2.0)	(1:4.0)

\*CNT-CCB ratio is clarified from the previous work [16]

mDES were labeled as ‘NR-C/mDES<sub>x</sub>’, where  $x$  refers to the DES content existing in mDES following the unit of part per hundred rubbers [phr]. The recipes of all composite samples are shown in Table 2.

### 3. Characterizations

#### 3.1. Cure characteristic

Cure characteristics of pure NR and NR/CNT-CCB composites with various mDES loadings were determined using a rubber process analyzer (RPA 2000, Alpha Technologie, Hudson, Ohio, USA). Each sample (1 sample of each formulation) was investigated at a fixed oscillation frequency (1.66 Hz) and amplitude (0.5° arc) at 160 °C. The curing properties were reported as scorch time ( $t_{s2}$ ) (the time at which the torque has increased by 2 dN·m from the minimum torque *i.e.* the initiation of chemical crosslinking), curing time ( $t_{c90}$ ) (the time at which the molecular chains have reached 90% of chemical crosslinking propagation) and the torque difference ( $M_H - M_L$ ) (the different of maximal ( $M_H$ ) and minimal ( $M_L$ ) torques).

#### 3.2. Payne effect

To investigate the Payne effect of pure and conductive NR composites, a rubber process analyzer (RPA 2000, Alpha Technologies, Hudson, Ohio, USA) at 100 °C was used. The test was performed under shear deformation with strain amplitudes in the range of 0.56–100% at a fixed oscillation frequency (1 Hz) to analyze the storage shear modulus ( $G'$ ) of each sample (1 sample of each formulation). The Payne effect was calculated by Equation (1):

$$\text{Payne effect: } \Delta G = G'_{0.56} - G'_{100} \quad (1)$$

where  $G'_{0.56}$  and  $G'_{100}$  are the storage moduli at 0.56 and 100% strain amplitudes, respectively. It is noted that the high Payne effect value indicates the reduction in strength of the filler network.

#### 3.3. Electrical properties

The electrical properties of the samples in terms of resistance ( $R_p$ ) were measured at room temperature using an LCR meter (E4980A, Keysight Technologies, Inc., Santa Rosa, California, USA). Approximately 2 mm thick samples were placed between two parallel plates of a dielectric test fixture (16451B dielectric test fixture, Keysight Technologies, Inc., Santa Rosa, California, USA) with a 38 mm electrode diameter. The analysis was performed over the frequency range from 20 to 100 kHz, and 5 different points of each sample were tested. The electrical conductivity ( $\sigma$ ) was calculated using Equation (2) [29]:

$$\sigma = \frac{1}{\rho} = \frac{d}{(R_p)A} \quad (2)$$

The parameters  $d$  and  $A$  refer to the sample thickness and the area of an electrode, respectively. The factor  $\rho$  is the volume resistivity, *i.e.*, the reciprocal of conductivity.

#### 3.4. Tensile properties

Tensile testing was performed using the dumbbell-shaped specimens of composites according to ISO 527 (type 5A) using 5 different samples for each formulation. The stress-strain behavior of the composites was then studied using universal testing machines (Model 3365, Instron® Inc., Norwood, Massachusetts, USA) operated at a crosshead speed of 200 mm/min at room temperature (25±3 °C).



### 3.5. Piezoresistive properties

The piezoresistivity was investigated using a universal testing machine ZwickRoell Z005, (ZwickRoell, Ulm, Germany), with an integrated source meter Keithley 2450 (Keithley Instruments, Solon, USA) with 3 different samples for each formulation. To record the electrical signal during mechanical test, the source meter was connected to a computer, and KickStart software (Keithley Instruments, Solon, USA) was used for data storage. The electrical resistance was calculated by the measured current, while the voltage was held constant at 1 V, as seen in the setup instrument in Figure 1. From the resistance analysis, the relative resistance ( $R_{rel}$ ) was calculated following Equation (3), where  $R$  is the measured resistance and  $R_0$  is the initial resistance, measured after fixing the sample inside the universal testing machine. The 5 bar pneumatic pressure was applied on the insulation grips to avoid slippage.

$$R_{rel} = \frac{R - R_0}{R_0} \quad (3)$$

In addition to the tensile test, cycling and quasi-static tests were performed to investigate the sensor behavior of conductive NR composites (CNRC) in detail. All the tests were performed at room temperature with a crosshead speed of 50 mm/min. The

dumbbell-shaped specimen (ISO 527, type 5A) was inserted between the grips aligned with the direction of extension. The dynamic tests were performed with 20 cycles (strain loading and releasing). The quasi-static tests were performed by stretching and releasing the samples with a dwell time of 60 s at minimal and maximal strain. Both dynamic and quasi-static tests were performed between 0–50 and 50–100% strain levels. Further details on the dynamic and quasi-static analysis of soft sensor materials are reported elsewhere [30–34].

## 4. Results and discussion

### 4.1. Processability and network formation in NR composites with DES

#### Ability to perform NR product

Figure 2 shows the crosslinking propagation of NR composites with various mDES (aZnO:DES) ratios. The vulcanization properties in terms of  $M_L$ ,  $M_H$ ,  $M_H - M_L$ ,  $t_{s2}$ , and  $t_{c90}$  are summarized in Table 3. The NR composites with mDES at the aZnO:DES ratio 1:1 exhibited the highest  $M_H$  due to improvement of filler dispersion with using mDES. The  $M_H$  steadily decreased with increasing aZnO:DES ratios because the excess of mDES considerably acts like a lubricating plasticizer in the NR compound [35]. A higher amount of DES in mDES reduces NR

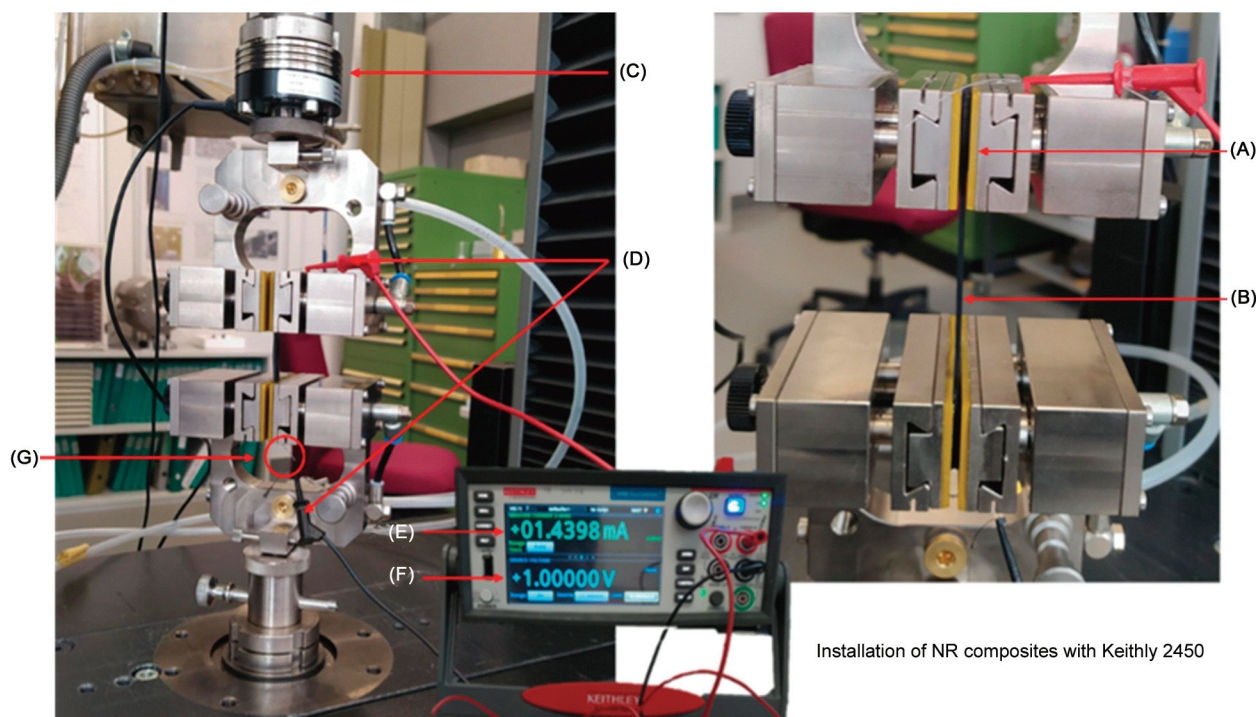


**Figure 1.** Universal testing machine with integrated piezoresistive analysis, pneumatic clamping and electrical connection of the conductive NR composite samples, where (A) – Insulation clamp, (B) – Rubber sample, (C) – Load cell, (D) – Conduction clamp, (E) – Electrical/Resistance detection, (F) – Applied voltages and (G) – Conduction wire.

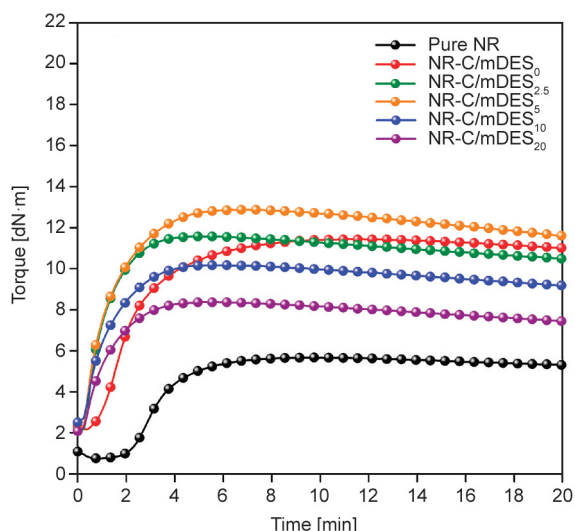


**Figure 2.** Vulcanization curves of pure NR and conductive NR composites (CNRC) with various mDES ratios. Up to 5 phr of mDES, the torque and the value of  $M_H - M_L$  are increased. This can be correlated with the increased crosslink density. A further increase results in lowering torque value and crosslinking density.

chain entanglement, which develops strong molecular chain slippages and higher mobilities in the composite; hence it lowers the value of  $M_H$ . Considering the  $t_{s2}$  and  $t_{c90}$  of the NR composites in Table 3, both properties are significantly decreased upon increasing the amount of mDES. This is due to the formation of ionic interaction between NR and DES molecules [16]. Molecular chain degradation of NR occurs during compression molding, which results in the formation of ketone functional groups at the terminal chain of NR [36, 37] and the promotion of new ionic linkages between NR and DES molecules. Thus, active C=C bonds in NR are decreased and accelerate the vulcanization of conductive NR composites. Additionally, it can be observed that up to 5 phr of mDES in NR compounds, the value of  $M_H - M_L$  dramatically increased. This is related to the enhancement of crosslink density (inferred from

$M_H - M_L$ ) based on the newly formed links of NR-mDES-CNT, NR-mDES-CCB, and NR-mDES-CNT-CCB. The proposed ionic interaction mechanisms in NR/CNT-CCB composites filled with DES are shown in Figure 3. At a higher loading level of mDES, the value of  $M_H - M_L$  steadily decreased due to the formation of filler agglomerates or the micro-phase separation of mDES in the NR compounds, which resulted in a reduced force of attraction between the linkages. It can be concluded that the proper addition of mDES improves the processing of NR composites by reducing  $t_{c90}$  and increasing the estimated crosslink density based on  $M_H - M_L$ .

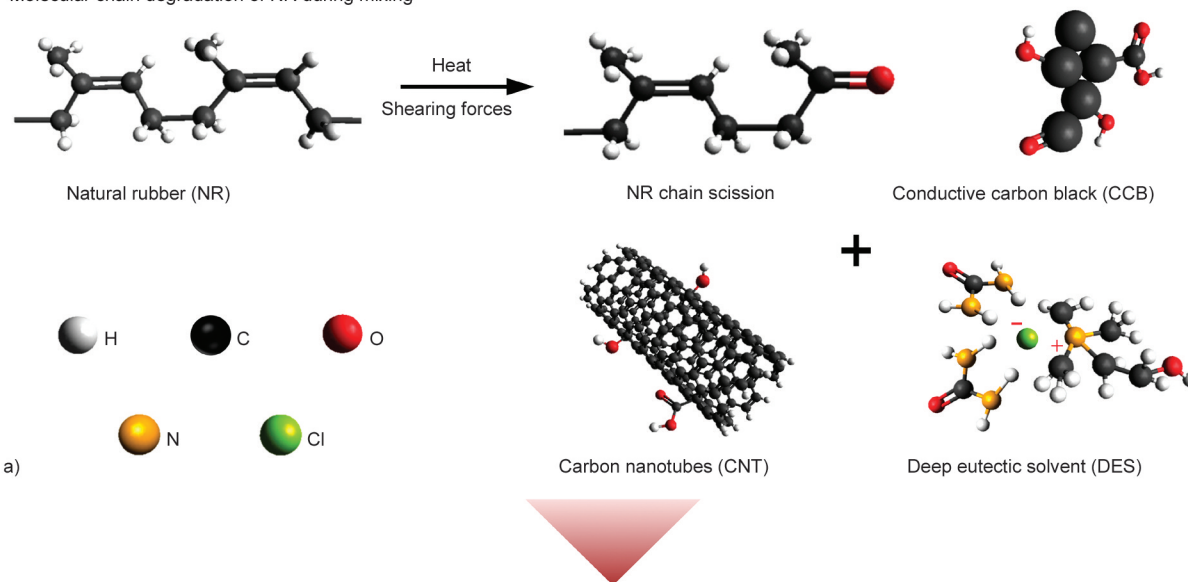
#### Formation of conductive network

The formation of CNT-CCB network in NR composites upon the addition of various mDES loading was examined from the electrical conductivity, which directly relates to the degree of filler dispersion [38]. Figure 4 shows the electrical conductivity as a function of frequency for the pure NR and CNRCs. As expected, the conductivity of the resulting material depends on the applied frequency. The electrical resistivity of pure NR and CNRC without mDES indicated poor transport of electric charges throughout the composites. For NR and CNRC, this is due to the insufficiently connected filler networks in the rubber matrix [38], as displayed in the proposed model (Figure 5a). In the case of CNRC without mDES, conductivity monotonically increases at a frequency below  $10^4$  Hz. This is attributed to the tunneling of electrons from end to end of CNT/CCB networks which increases with frequency. For the CNRC with mDES, conductivity is less dependent on the frequency because of the occurrence of electronic and ionic conduction inside the NR matrix. With the proper mDES, wetting of the liquid region on CNT/CCB surfaces helps to transport the electronic charges and improves the conductivity. Simultaneously, ionic charges move through the newly formed mDES pathway and can change the electrical behavior of the composites. Composites with 2.5–5.0 phr mDES, the partly wetted CNT-CCB surfaces by mDES, as seen proposed model in Figure 5b, accelerate the charge carriers through the CNT-CCB combination and support the network formation with narrow filler-filler contacts leading to an increase in conductivity of composites based on electron tunneling along the end-to-end of CNT-CCB [39]. This means that mDES develops a molecular chain bridge among the

**Table 3.** Crosslink properties of NR and CNRC with various mDES ratios.

Samples	Cure characteristics				
	$M_L$ [dN·m]	$M_H$ [dN·m]	$M_H - M_L$ [dN·m]	$t_{s2}$ [min]	$t_{c90}$ [min]
Pure NR	0.7	5.6	4.9	3.0	5.4
NR-C/mDES <sub>0</sub>	2.1	11.4	9.3	1.3	5.2
NR-C/mDES <sub>2.5</sub>	2.1	11.6	9.5	0.5	3.5
NR-C/mDES <sub>5</sub>	2.1	12.9	10.8	0.4	3.3
NR-C/mDES <sub>10</sub>	2.5	10.2	7.7	0.5	2.9
NR-C/mDES <sub>20</sub>	2.1	8.5	6.4	0.6	2.7

Molecular chain degradation of NR during mixing



The proposed ionic interaction mechanisms in CNT-CCB based CNRC with mDES

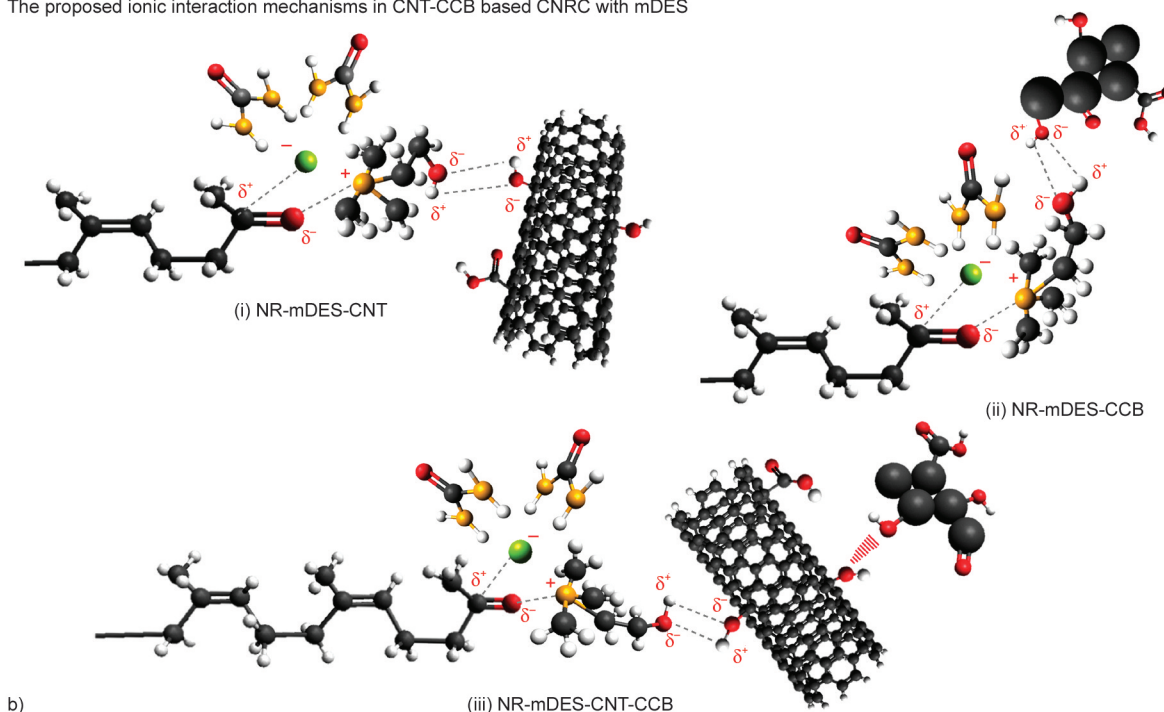


**Figure 3** Proposed models of ionic interaction mechanisms in CNT-CCB based CNRC with mDES. a) Molecular chain degradation of NR during mixing generates ketone functional groups at the terminal chain of NR. b) The proposed ionic interaction mechanisms are shown as (i) NR, mDES, and CNT, (ii) NR, mDES, and CCB, and (iii) NR, mDES, and CNT/CCB.

filler particles. Hence, better electron transport takes place throughout the composites, resulting in the improved electrical conductivity of the composites. Below 5.0 phr of mDES, the effect of electronic conductivity is more predominant than the conductivity contributed by ionic charge transportation. However, beyond 5 phr of mDES (Figure 5c), the formation of mDES region occurs in the NR matrix. Thus, the conductivity arises in the composite due to two different

forms of networks. Generally, at higher frequencies, the electronic conductivity increases by reducing the ionic conductivity [40, 41]. The excess of mDES results in lowering the electrical conductivity. However, the excess of DES not only affected the conductivity but also imposed on the percolation threshold concentration of the composites. In this case, we have modified the percolation threshold theory for finding the critical DES concentration ( $\rho_{CX}$ )



that enables the suitable electrical conductivity of NR composites. In general, the  $\rho_{CX}$  is examined from the plot of electrical conductivity and the varied chemical content (*i.e.*, amount of DES). With the curves, the  $\rho_{CX}$  of the composites can be evaluated using the classical percolation theory as Equation (4) [42]:

$$\sigma = \sigma_0(\rho - \rho_{CX})^t, \rho > \rho_{CX} \quad (4)$$

where  $\sigma_0$  is a constant value,  $\rho$  is the DES ratio in mDES and  $t$  is the scaling exponent. As observed in the inset of Figure 4, the fitting results show that a low  $\rho_{CX}$  of DES ratio in mDES is found at 0.24 in conductive NR composites with mDES. This indicated the formation of an interconnected conductive network throughout the NR phases. It clarifies well that the addition of a little DES ratio in mDES improved well dispersion of CNT-CCB hybrid filler in the NR composites and consequently increased the electrical conductivity of the conductive NR composites.

The state of CNT-CCB dispersion and distribution in the NR matrix can also be observed from the relation of storage moduli of the composites at maximal and minimal strain amplitudes which is the so-called Payne effect [43]. The value is directly related to the degree of CNT-CCB agglomerates in the matrix and also related to the strength of CNT/CCB network deformation [43]. Figure 6 shows the storage

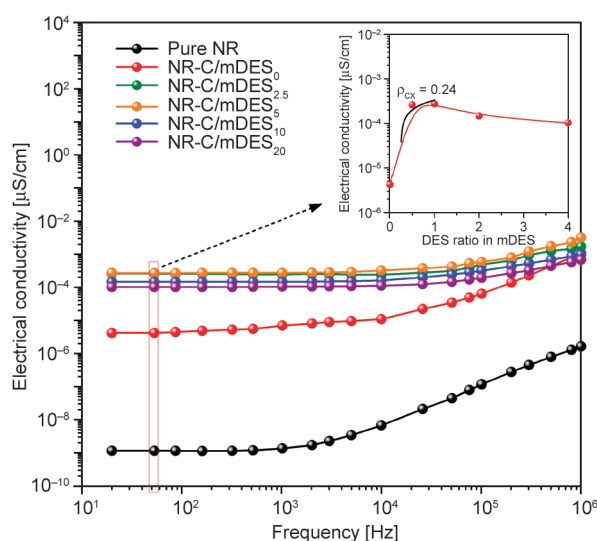


**Figure 4.** Electrical conductivity as a function of frequency for pure NR and their composites with various mDES ratios and the plot of electrical conductivity at a frequency of 50 Hz as a function of DES concentration in mDES to find the critical DES concentration ( $\rho_{CX}$ ) from the applied percolation threshold theory.

modulus as a function of strain amplitude which demonstrates that the incorporation of mDES up to the ratio of 1:1 (aZnO:DES) increases the storage modulus of NR composites. It improves the CNT-CCB dispersion in the NR matrix, relating the concentration over the  $\rho_{CX}$  value. As expected, at mDES ratio higher than 1:1, the initial storage modulus steadily decreased due to the excess of liquid phases inside the NR, which reduces the physical interactions from bound rubber absorption of NR molecular chain on the CNT-CCB surfaces, allowing the NR chains slippage and disentanglement. It also affects the strength of the CNT/CCB network, which can be broken easily upon the addition of excess mDES. Considering the Payne effect in Figure 6, a reduction in their values is found for the NR composites with mDES relative to the ones without mDES. This is contributed by the improved dispersion of CNT-CCB in rubber matrices, as described in models in Figure 5. The use of mDES reduced the degree of CNT-CCB agglomeration in the NR matrix, relating to the reduced Payne effect value. It also helps the CNT-CCB interconnection and supports the strength of network formation with narrow filler-filler contacts (as seen in Figure 5b). However, the addition of excess mDES lowers the Payne effect, and it is reflected in the poor  $G'$  values. This means that the increase of liquid phase inside the NR matrix improves the filler dispersion, but the network strength is worth it due to the ease of breakages under strain. Thus, it summarizes that the addition of proper mDES improves the dispersion very well and supports the network formation of CNT-CCB hybrid filler in NR composites by increasing the electrical conductivity of NR composites.

#### Effect of DES on mechanical properties

Network formation of CNT-CCB also affected the tensile properties of CNRC upon the addition of mDES. Figure 7 shows the stress-strain curves of pure NR and NR composites with various mDES ratios. Also, properties in terms of 100 and 300% moduli, tensile strength, and elongation at break are shown in Table 4. Pure NR shows a dramatic increase in the modulus at high strain (500–700%) due to strain-induced crystallization of NR molecules. However, CNRC with various mDES displayed higher initial slopes (*i.e.*, Young's modulus, the ability to resist the deformation of composites) and the moduli at 100 and 300% strains compared to pure

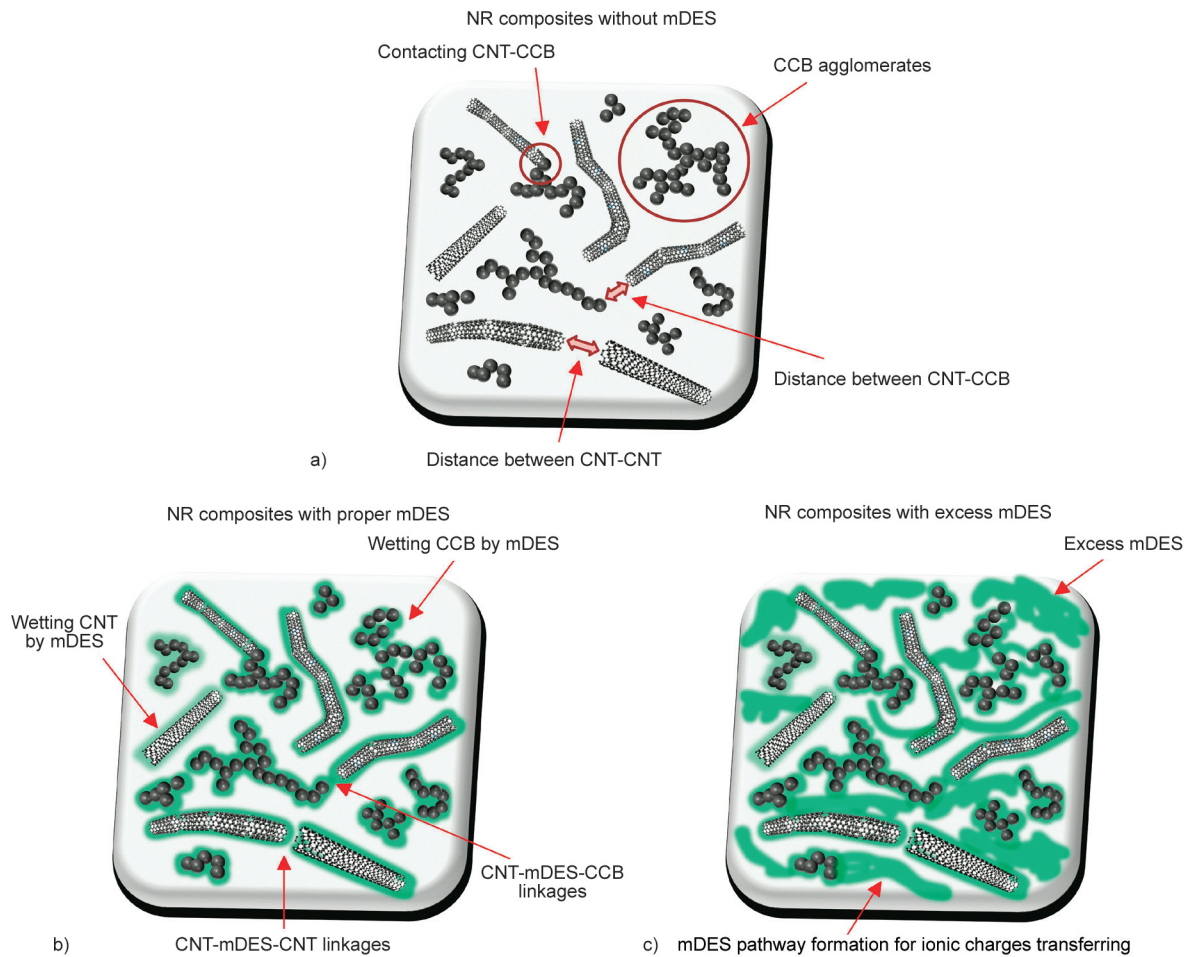


**Figure 5.** Proposed models of CNT-CCB dispersion inside the NR matrix; a) CNRC without mDES indicated poor electric transport due to a lack of connected filler networks in the rubber matrix, b) CNRC with proper mDES exhibited partly wetted CNT-CCB surfaces by mDES accelerates the network formation with narrow filler-filler contacts increases the conductivity and c) CNRC with the excess of mDES regions inside NR matrix.

NR. It is noted that the ‘modulus’ refers to the stiffness of a material that resists deformation. Thus, the addition of highly rigid filler particles into the NR matrix is expected to improve the stiffness of the composite. In contrast, higher stiffness leads to lower elasticity, and the composites exhibit lower strain at break. This can be explained by the surrounding CNT-CCB particles that strongly hinder the mobility of rubber chains [44]. Table 4 shows that the tensile strength of NR-C/mDES0 composites increases approximately 11% upon the addition of DES at the ratios 1:0.5 and 1:1 (aZnO:DES). The addition of sufficient mDES loading improved the dispersion of CNT-CCB in the NR matrix and increased the reinforcement efficiency of filler particles to rubber molecules. However, as seen in the proposed model of Figure 5c, increasing mDES above 5 phr increases the defect points inside the NR matrix and reduces the resistance of physical deformation during extension [45]. Thus, tensile strength is found to be strongly

lowered. In addition, the presence of excess liquid phases is observed in the morphologies of the composites, as seen in Figure 8. It is clearly noticed that the degree of filler agglomeration (*i.e.*, the purple area) is effectively increased upon increasing the loading level of mDES. Interestingly, in NR-C/mDES<sub>2.5</sub> and NR-C/mDES<sub>5</sub>, a homogenous dispersion of mDES in the NR composites filled with CNT-CCB is observed, especially the one with 5 phr of mDES compared to the one without mDES. A further increase in mDES results in a larger area of filler agglomeration.

According to the observed results of CNRC filled with various mDES loading, it is found that the addition of 5 phr mDES improves the processability of NR-C/mDES0 by reducing cure time and increasing tensile properties. However, excess DES from 10 and 20 phr reduces the properties of the composites owing to the existence of large defect regions. This leads the composites to break easily, and therefore,

R1  
R2  
R3  
R4  
R5  
R6  
R7  
R8  
R9  
R10  
R11  
R12  
R13  
R14  
R15  
R16  
R17  
R18  
R19  
R20



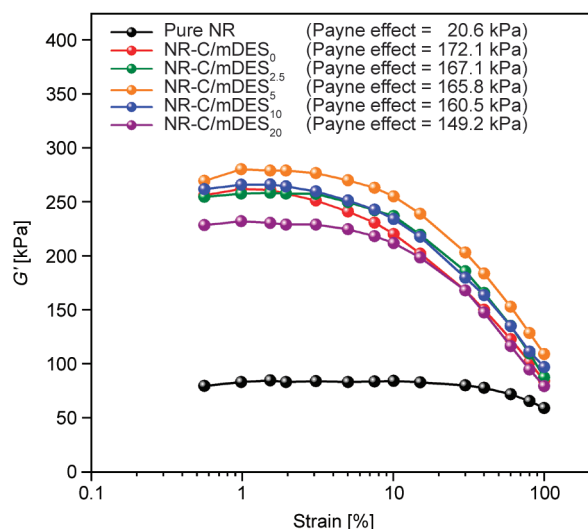


**Figure 6.** Relation of storage modulus and strain amplitude of pure NR and their composites with various mDES ratios. The test was performed under the shear deformation with strain amplitudes in the range of 0.56–100%. The obtained Payne effect from different storage moduli at 0.56 and 100% strain amplitudes, which refers to the strength of the filler network and filler dispersion inside the NR matrix, is also presented.

the tensile properties are decreased. Thus, the possibility of using the resulting composites as a motion sensor in soft actuators and piezoresistive properties

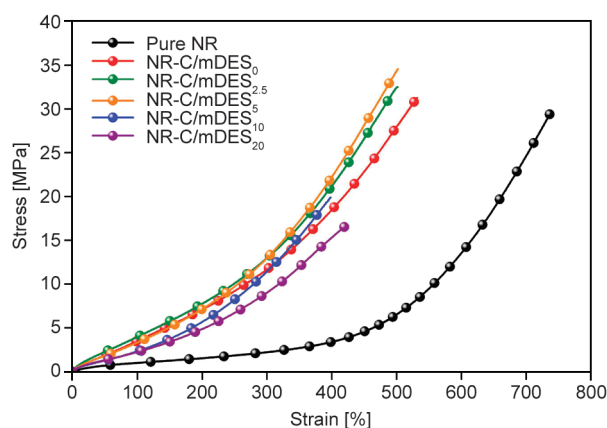


**Figure 7.** Stress-strain curves of pure NR and their composites with various mDES ratios.

**Table 4.** Tensile properties in terms of 100 and 300% moduli, tensile strength, and elongation at break of NR composites with various mDES ratios.

Samples	100% modulus [MPa]	300% modulus [MPa]	Tensile strength [MPa]	Elongation at break [%]
Pure NR	0.9±0.1	2.2±0.2	29.5±2.0	738.5±13.3
NR-C/mDES <sub>0</sub>	3.3±0.2	10.9±0.2	31.3±2.3	532.3±15.1
NR-C/mDES <sub>2.5</sub>	3.9±0.3	12.8±0.3	32.4±1.7	503.8±22.6
NR-C/mDES <sub>5</sub>	3.5±0.3	12.8±0.3	34.6±1.9	502.7±20.1
NR-C/mDES <sub>10</sub>	2.4±0.2	11.9±0.2	19.9±2.5	419.1±17.8
NR-C/mDES <sub>20</sub>	2.1±0.2	8.6±0.3	16.5±1.2	398.2±16.7

in terms of the relative change of resistance ( $R_{rel}$ ) by dynamic and quasi-static tests are investigated and further explained by matching with the proposed phenomena.

## 4.2. Piezoresistive properties of NR composites with mDES

### Sensitivity of the composites

The piezoresistive properties of the CNRCs are measured based on the variation of conductivity upon the application of stress by using a universal tensile testing machine. On straining the CNRC samples, the distance between conductive fillers increases, and electron transport is reduced by a larger distance between the fillers (tunneling effect). As a result, only CNRC samples without mDES and with 5 phr mDES are selected for sensor studies. Due to the considerable difference in the initial conductivity of these two samples (see Figure 4), the  $R_{rel}$  during tensile testing of the samples is shown in Figure 9. Both the CNRC samples show positive piezoresistive behavior. This can be explained by the loss of contact between the filler particles that results in enlarged electron tunneling resistance [42, 46, 47]. For piezoresistive strain sensors, the estimation of sensitivity correlates with the estimation of the gauge factor ( $GF$ ). It can be defined as the ratio of change in relative resistance to the change in strain. In this case, the correlation of both properties is linear; the  $GF$  is calculated from the slope of the plot of the relative resistance change and the applied strain of 0–50, 50–80, and 80–100% (see the estimated slope from the green line). A higher  $GF$  corresponds to a larger change in resistance at a given strain, and therefore it indicates good sensitivity [48]. In Figure 9, it is seen that the  $GF$  value of the CNRC with and without mDES had no significant differences relating to the applied strain of 0–50%. However, at 50–80 and 80–100% strain, the  $GF$  of the CNRC filled with mDES had approximately 2 and 4 times higher than

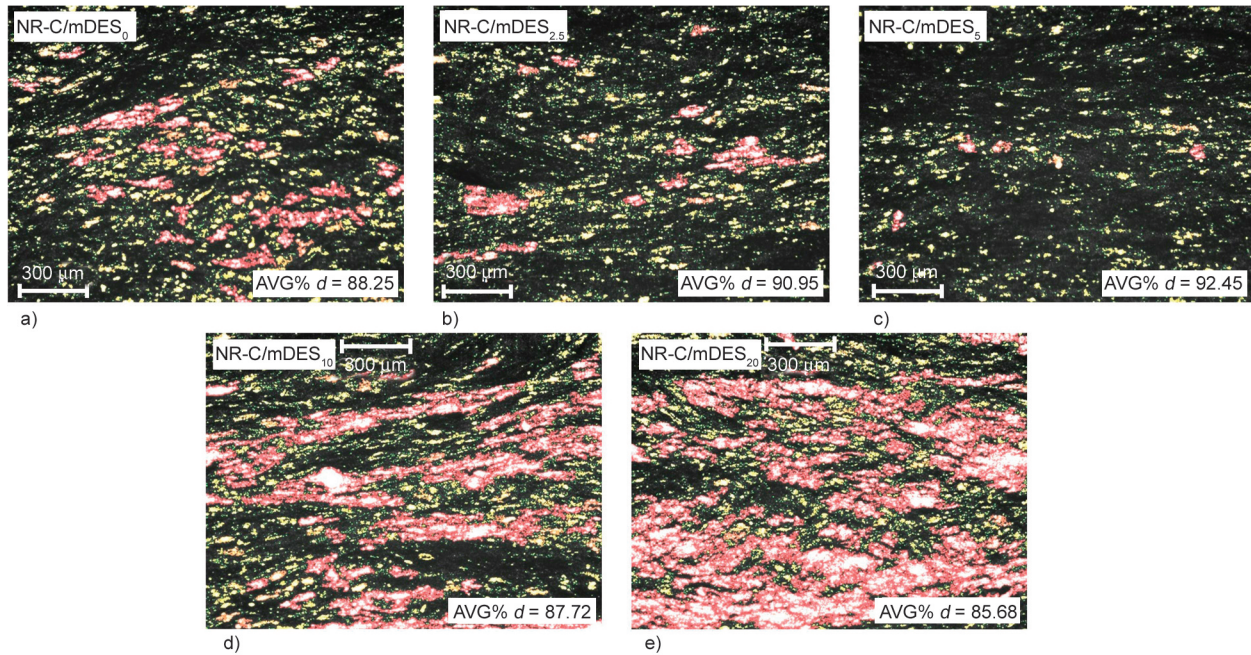


**Figure 8.** The morphologies based on optical microscope detection of the CNRCs with various mDES contents at 0, 2.5, 5, 10, and 20 phr, respectively, using a magnification of 100 $\times$ . The purple area refers to the agglomeration areas of the fillers, whereas the AVG%  $d$  is the average% dispersion of the filler inside the NR matrix. a) NR-C/mDES<sub>0</sub>, b) NR-C/mDES<sub>2.5</sub>, c) NR-C/mDES<sub>5</sub>, d) NR-C/mDES<sub>10</sub>, e) NR-C/mDES<sub>20</sub>.

that of one without mDES. This clarifies the fast responsibility of the composites due to the addition of the DES, reflecting good sensitivity at the applied strain. Thus, at 0–50% strain, similar  $GF$  is received and not applicable for interpreting the sensitivity of the CNRC. In addition, the sensitivity of the presented CNRC to other conductive composites is based on the TPU, SR, and PDMS matrices indicated in Table 5. It is clearly seen that the NR-C/mDES<sub>5</sub> had

the highest maximal  $GF$  value relative to the others used matrices. The two different reasons for the obtained results are related to (i) the high molecular weight of NR, which causes superior elasticity to the material, and (ii) the long molecular chain of NR, which provides a high degree of chain entanglement that resists breakage of the material. This is also the phenomenon for affirming the sensing performance of the CNRC owing to the addition of the mDES.

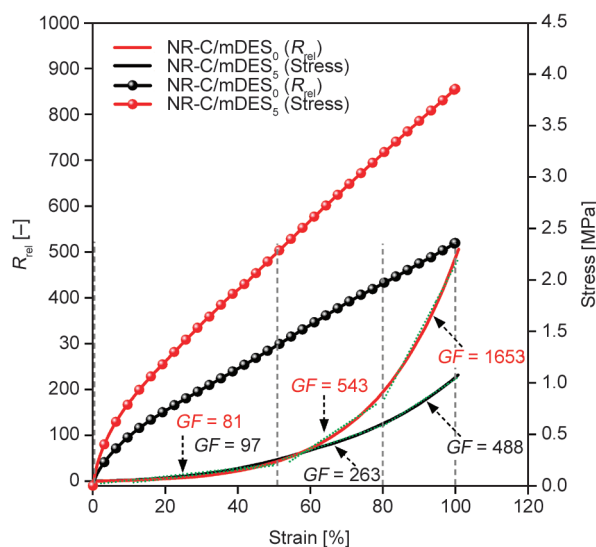


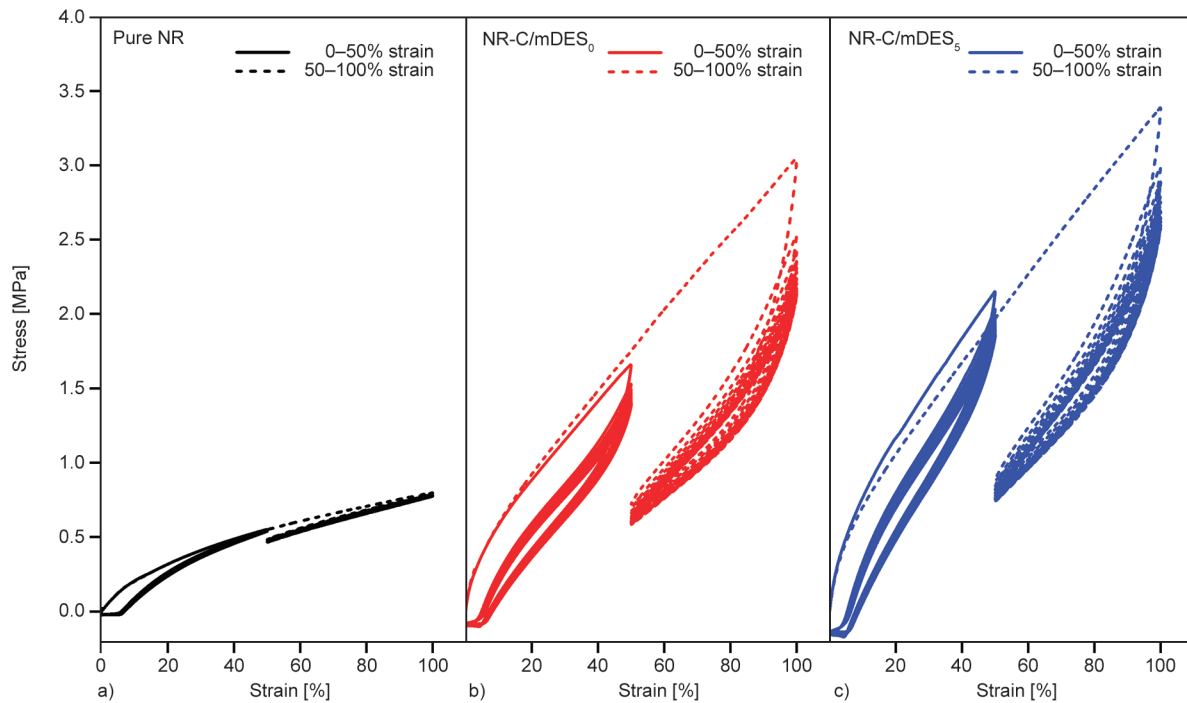
**Figure 9.** Relative resistance ( $R_{rel}$ ) and stress as a function of strain together with the  $GF$  values calculated from the slope of the plot of  $R_{rel}$  changes at 80–100% strain.

### Cyclic testing

Dynamic testing provides useful insights into the sensing behavior of the long-term performance of a composite sensor system [42]. Dynamic cyclic tests are performed to ensure the sensor signal's repeatability under the given strain [53]. This indicates the linearity of the sensor signal response during loading and unloading, the signal drift, and the reliability of the sensor in terms of how the signal response changes after many consequent cycles of loading and unloading. Figure 10 shows the variation of stress-strain curves in the case of pure NR and CNRC with and without mDES. The samples have been cycled 20 times from 0–50 and 50–100% strains. It is found that the CNRCs showed lower stress during 2<sup>nd</sup> cycle than the 1<sup>st</sup> cycle of the dynamic test when compared to pure NR. This is attributed to the detachment of rubber from filler surfaces as a result of poor filler

**Table 5.** Sensing performance comparison of the CNRC with and without the addition of DES relative to other referenced matrix composites, where <sup>a</sup>, <sup>b</sup>, <sup>c</sup>, and <sup>d</sup> are assigned to thermoplastic polyurethane (TPU), reduced graphene oxide (rGO), polydimethylsiloxane (PDMS) and silicone rubber (SR), respectively.

Samples	Sensor type	Stretchability	Linearity	Maximal GF
NR-C/mDES <sub>0</sub>	Resistive	100%	Three linear regions	488.0
NR-C/mDES <sub>5</sub>	Resistive	100%	Three linear regions	1653.0
TPU <sup>a</sup> /rGO <sup>b</sup> [50]	Resistive	100%	Two linear regions	79.0
PDMS <sup>c</sup> /CNT [51]	Resistive	100%	Two linear regions	87.0
SR <sup>d</sup> /GP [52]	Resistive	12%	Two linear regions	164.5

**Figure 10.** Stress-strain curves of pure NR and their composites without and with mDES during the 20 cycles of the dynamic tensile testing at 0–50 strain and 50–100% strain. a) Pure NR, b) NR-C/mDES<sub>0</sub>, c) NR-C/mDES<sub>5</sub>.

reinforcement efficiency. However, comparing the composites, the sample with mDES exhibited higher stress than without mDES. It is expected that the incorporation of mDES causes improvement in the dispersion of CNT-CCB hybrid fillers which subsequently increased the reinforcement efficiency in the NR matrix.

For the investigation of signal drift under strain, the maximum stress of each cycle ( $\sigma_{\max-C_y}$ ) needs to be examined. Here, the difference in  $\sigma_{\max-C_y}$  at the first cycle of the one without and with pre-straining is due to the detachment of NR molecules from the filler surface, which is increased with the degree of extension ratio. Based on the  $\sigma_{\max-C_y}$  of the composites with and without mDES, it is found that the addition of mDES significantly helped the composites by lowering the % change of  $\sigma_{\max-C_y}$  along with the cyclic testing. This correlated well to the relation of stress-time

curves at 0–50 and 50–100% indicated in Figures 11e–11h. In addition, to examine the effect of DES on the hysteresis of the NR composites, the difference of  $\sigma_{\max-C_y}$  and  $\sigma_{\min-C_y}$  (*i.e.* minimum stress of each cycle) is known as the correlation of the estimated hysteresis of the CNRC was interpreted. It is seen that the larger different values are found after the addition of DES. This means that the NR-C/DES<sub>5</sub> composite had higher energy dissipation than the one without DES during the help of DES phase, which causes improvement of reinforcement efficiency relating well dispersion and distribution of fillers throughout the NR matrix.

Considering the variation of  $R_{\text{rel}}$  value upon applying and releasing strain, the different  $R_{\text{rel}}$  behaviors of NR composites under loading and unloading cycles at 0–50 and 50–100% strains are shown in Figures 11a–11d. In Figure 11, the  $R_{\text{rel}}$  of the composites exhibited



a decreasing trend as the number of cycles increased, and this reduction in resistivity was more pronounced at the beginning of the test. A decrease in  $R_{rel}$  is

observed during the cyclic test caused by softening of the matrix due to the breakage of filler-filler contacts and the detachment of NR molecules from

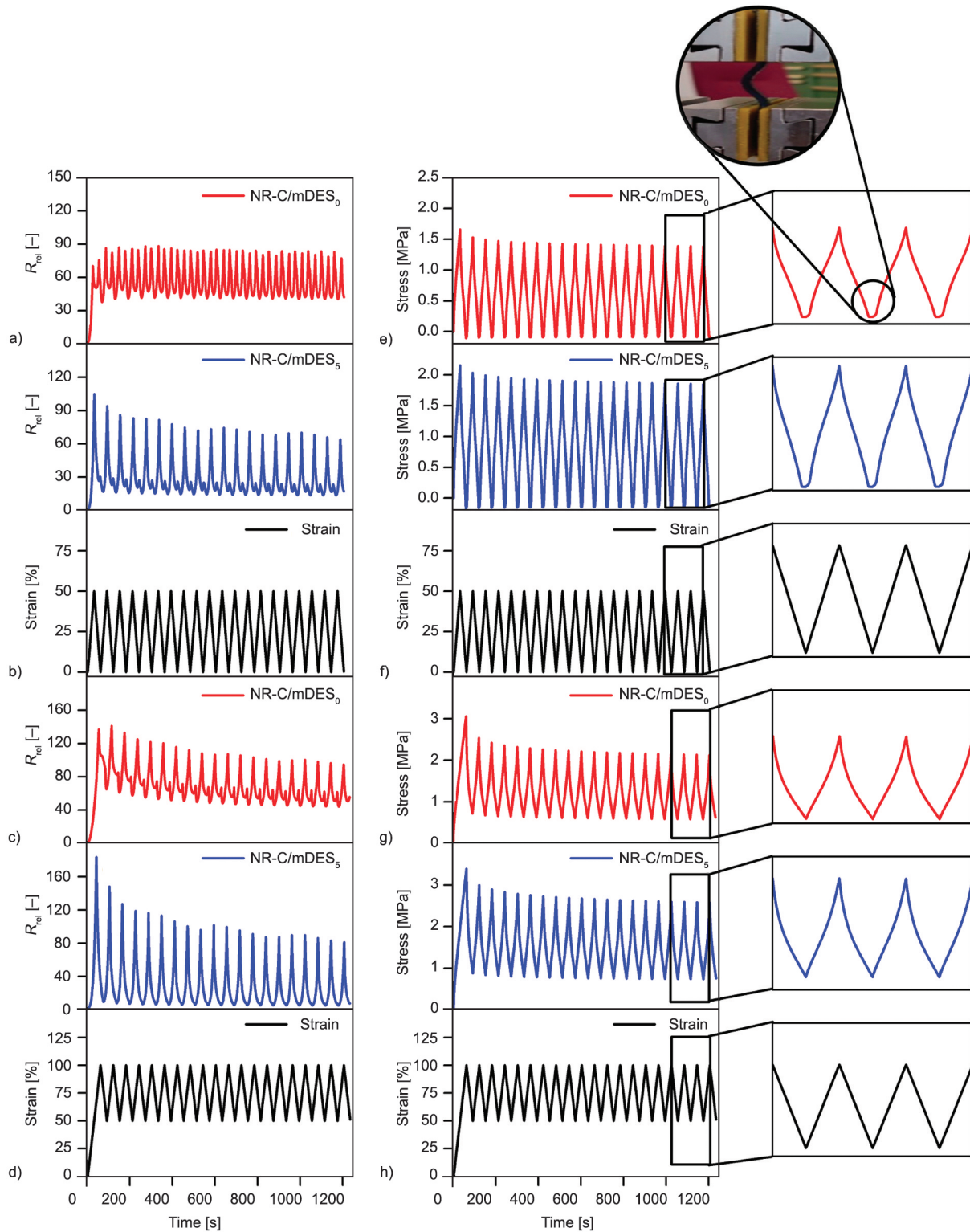


**Figure 11.** Variation of  $R_{rel}$  value upon applying and releasing strains of a) CNRC without mDES, b) CNRC with 5 phr mDES together with the relation of stress and time of e) CNRC without mDES and f) CNRC with 5 phr mDES on performing the dynamic tests in 20 cycles at 0–50% strain. Also,  $R_{rel}$  and stress changes as a function of time during the dynamic tests at 50–100% strain of CNRC without and with mDES 5 phr are shown in c), d), g), and h), respectively.

CNT/CCB surfaces [13, 41]. Repeated stretching and contracting during the cyclic strain test increase the contact surface areas of the existing conductive particles due to the occurrence of multiple contacts of each particle. At the same time, the additional conductive pathways established during stretching and releasing reduce the electrical resistance [42, 54]. In addition, it is also seen in Figure 11 that the resistivity of the composites increased upon the application of mechanical force because of the change in distance of separation between the particles, and further, the resistivity is found to be decreased with strain. This is typical behavior of piezoresistive composites known as the positive strain effect or positive response. However, the further contraction (*i.e.*, decreasing strain) results in increasing resistance, leading to an additional peak in each cycle. This peak exhibited a negative strain effect that has already been reported in the literature [2, 49]. The existence of a shoulder peak or a negative response during loading-unloading cycles indicates the formation of destruction and reconstruction of conductive pathways [55, 56]. Also, buckling of the sample, as shown in Figure 11e, was another reason for the more pronounced shoulder peak. However, in Figure 11b, the composites with mDES exhibited a smaller negative effect on the peak as compared to the composites without mDES (Figure 11a). This can be related to the

synergy of plasticizing by mDES that provides better dispersion of CNT-CCB hybrid fillers, originating infinite 3D CNT-CCB pathways inside the NR matrix. In addition, the partly wetted CNT by mDES accelerated the dispersion of CNT and supported the network formation with narrow filler-filler contacts that led to an increase in the conductivity of composites by reducing the shoulder peak. Figure 11d shows that the shoulder peak of NR composites at 50–100% strain was significantly decreased from the NR composites at 0–50% strain (Figures 11a and 11b). It can be related to the visco-elastic behavior of the composites upon changing the extension ratio and addition of mDES, as shown in the proposed mechanism (Figure 12). On increasing the extension ratio of the composites (Figure 12a), the detachment between NR molecules and filler surface has occurred, and therefore, the restriction of NR deformation is lowered. This phenomenon reduces the elastic nature of NR molecules to regain the original shape and finally decreases the buckling phenomena. Thus, the secondary peak of the electrical signal is found to be minimized. However, with no significant changes in the bending degree of the composites after releasing forces and the addition of DES eliminates the appearance of the unnecessary peak. In Figure 12c, it is seen that the wetting of DES on the surface of CNT-CCB indicates tunneling of current through the

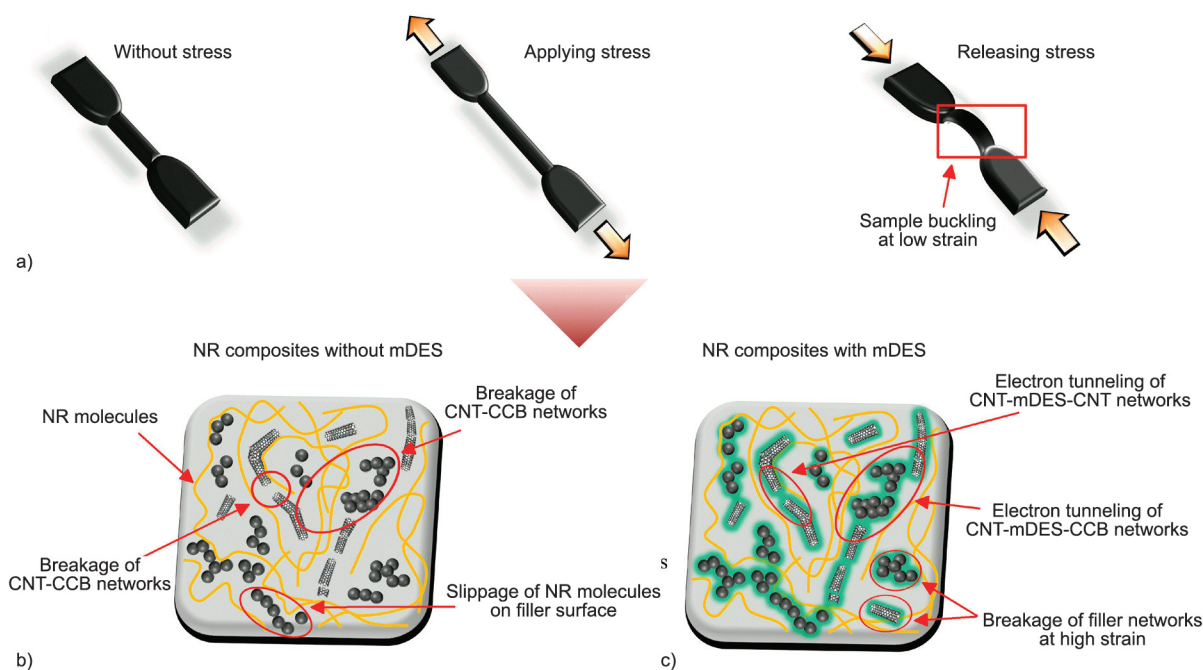


**Figure 12.** Proposed models of the CNRC without and with mDES during extension. a) Changes in the appearance of specimens during stretching and releasing. b) The proposed image of filler network formation of CNRC without mDES when applying stress. c) The schematic mechanism of mDES wetting on the CNT-CCB surfaces accelerated the CNT-mDES-CNT and CNT-mDES-CCB linkages in CNRC with mDES during extension.



linkages of CNT-DES-CNT and CNT-DES-CCB even though it consists of separation between them. Therefore, under dynamic conditions, the DES stabilized well the transport of electric current throughout the NR matrix and effectively minimized the signal errors.

#### Quasi-static testing

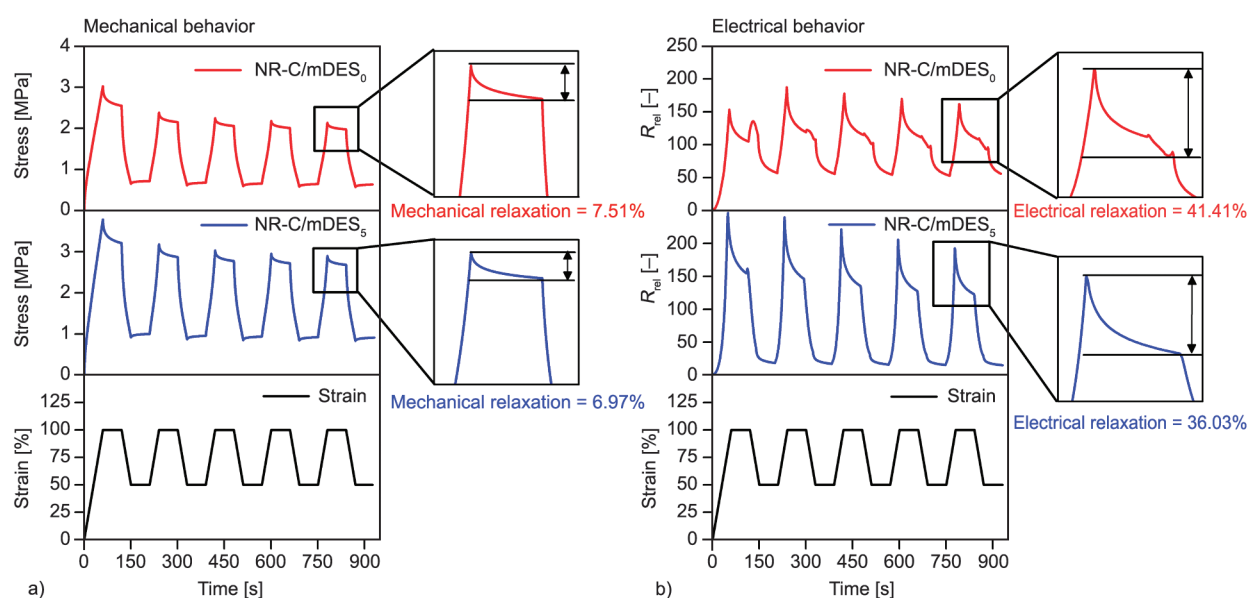
The applicability of CNRC with 5 phr mDES and without mDES has been studied in soft actuators. The sensor has to measure the same strain at different intervals of time. Rubber molecules are linked with stress relaxation phenomena that exhibit the effect of the piezoresistive response of the strain sensor [57]. Therefore, a quasi-static test can be conducted to study the effect of relaxation and drifts on the sensor performance due to the interconnection between the rubber-filler, where the stress is held constant with time [58]. Figure 13 shows the quasi-static results of NR composites with and without mDES focusing on stress and  $R_{rel}$  relaxation at constant strain and strain varying between 50–100%. In Figure 13a, it is seen that the stress relaxation is 6.9 and 7.5% in the cases of CNRC with and without mDES, respectively. This means that NR molecular chains and CNT-CCB particles with mDES build a more stable network, and it cannot be easily moved due to the better dispersion of filler in the NR matrix. The results correlated with the electrical relaxation represented in

Figure 13b. As expected, the value of  $R_{rel}$  increases on applying strain and decreases when the strain is lowered. When the strain is held at a constant ratio, the  $R_{rel}$  decreases to approximately 41.4% for the composite without mDES and 36.0% for the one with mDES. This reduction in relaxation of CNRC with mDES can be explained by molecular chain bridging among the filler particles by mDES, although the sample experiences buckling. As already mentioned, mDES helps the electron transport throughout the NR matrix by improving the electrical conductivity, and the CNRC composites with mDES<sub>5</sub> exhibited better sensor performance compared to others.

#### 4.3 Use of CNRC filled with mDES<sub>5</sub> to detect motion of the soft tendon-based actuator

##### Fabrication of soft tendon-based actuator

A soft tendon-based actuator has been designed with one joint (flexible hinge), as can be seen in Figure 14. Here, the tendon-based actuator was fabricated by fused deposition modeling (FDM), a method of material extrusion additive manufacturing. For the fabrication, A Raise Pro 2 FDM 3D printer from Raise 3D (Irving, Texas, USA) was used. The material used for the actuator was 1.75 mm TPU filament with Shore hardness 90A, supplied by Spectrum (Pecice, Poland). The temperature used during printing was 230 °C for the printing head and 45 °C for the printing



**Figure 13.** a) Mechanical behavior by means of stress as a function of time of the CNRC without mDES and with 5 phr mDES during the quasi-static testing. The tests were performed by stretching and releasing the CNRC in 50–100% strain together with a dwell time of 60 s at minimal and maximal strains. b) The  $R_{rel}$  signal relaxation behavior in a quasi-static strain cycling test of CNRC without mDES and with 5 phr mDES relative to time.

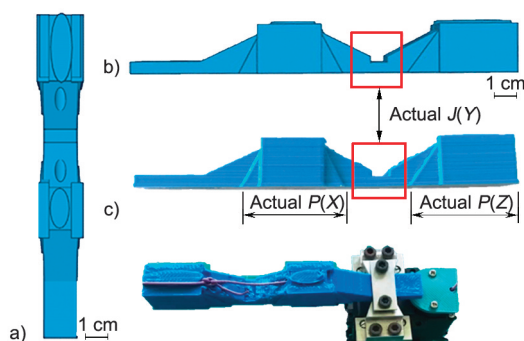


**Figure 14.** Computer-aided design (CAD design) of the soft tendon-based actuator for the top view (a) and side view of the design (b) and the printed material (c).

bed. The filament was printed with a speed of 20 mm/s and an extrusion multiplier of 1.2.

For the actuation, a tendon consisting of 0.3 mm copper wire coated with polytetrafluoroethylene was attached to a Dynamixel AX-12A servomotor from Robotis (Lake Forest, Illinois, USA). For the control of the servomotor, an Arduino Mega microcontroller with an external power supply was used. The actuator was programmed to move from open position to closed position with a 2 s delay in each position (Figure 14c).

#### *Sensing the motion of the tendon-based actuator*

To detect the motion of the tendon-based actuator, a dumbbell-shaped sensor was used, similar to the samples used in tensile testing experiments. The

CNRC was fixed on the actuator using Sil-Poxy glue from Smooth-On (Macungie, Pennsylvania, USA), as seen in the installation details (Figure 15). The CNRC sensor was connected with a multi-meter using electrical safety grippers to detect the motion of the actuator and the sensor signal, as shown in Figure 15 and Appendixes 1 and 2. It is seen that the monotonic sensor signal could be achieved. However, a significant drift could be observed owing to the breakage of filler networks and detachment of NR molecules from the CNT/CCB surfaces related to the extension of CNRC, as also found in the cyclic test displayed in Figure 11. Figure 15 shows no second peak even though it has been strained several times.

Therefore, the bending motion of a soft tendon-based actuator can be detected by the CNRC with 5 phr mDES. In an additional experiment, the actuator design and tendon material are changed, as shown in Figures 16. Based on these results, it can be proposed that the drift shown in Figure 15 is also affected by the actuator design and the tendon material. According to Figure 14, the design of the actuator is investigated by varying the thickness of the position at Actual  $J(Y)$ , which connects the Actual  $P(X)$  and  $P(Z)$  parts. Figure 16a shows the  $R_{rel}$  change of CNRC sensor fixed on the actuator with different thicknesses of Actual  $J(Y)$ , namely 2, 3, and 4 mm. It is seen that a similar monotonic sensor signal is represented for all different hinges, although the drifts are slightly

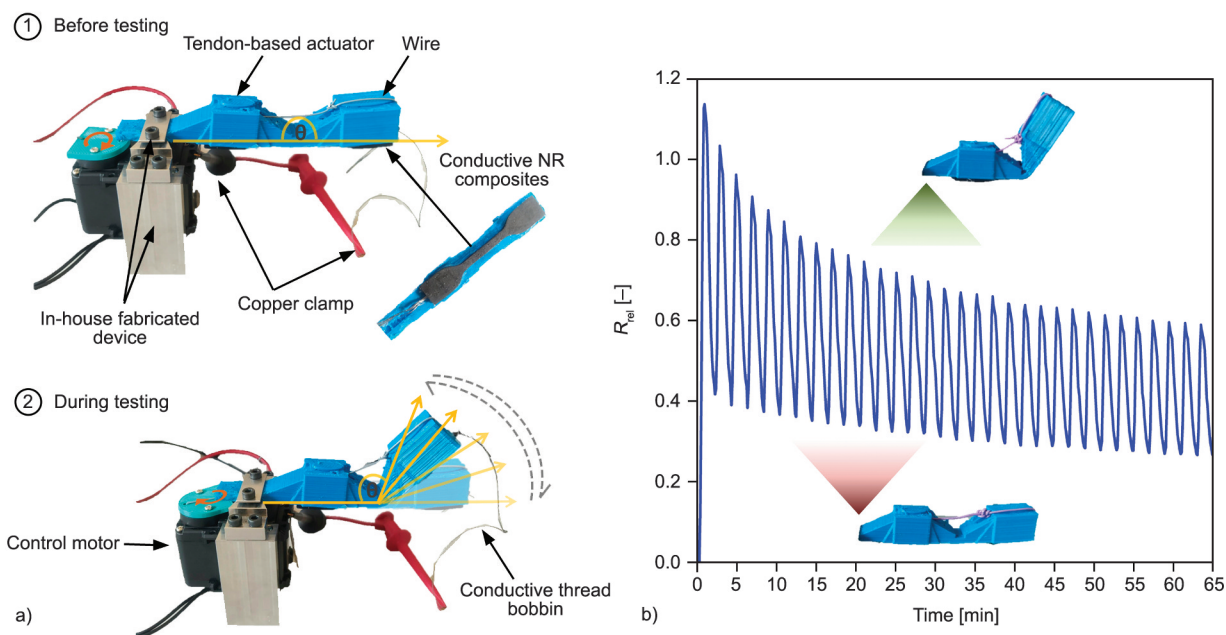


**Figure 15.** a) Steps of setting the tendon-based actuator with integrated CNRC sensor and b) the variation in resistance during the motion of the actuator.

different due to the difference in stress inside the hinge. **Figure 16b** shows the effect of the tendon cross section on the  $R_{rel}$ . The actuator with 3 mm of Actual  $J(Y)$  was chosen for the test with different cross sections and cladding types of metal tendons such as  $0.06 \text{ mm}^2$  (polytetrafluoroethylene, PTFE),  $0.14 \text{ mm}^2$  (thermoplastic elastomer, TPE (styrene-ethylene-butylene-styrene copolymer)),  $0.23 \text{ mm}^2$  (polyvinyl chloride, PVC) and  $0.35 \text{ mm}^2$  (PVC). It is observed that the different tendon types exhibited slightly different drifts within the cyclic sensor signal. Also, in the case of PVCs with smaller tendon cross-sections, the greater  $R_{rel}$  changes of the CNRC sensors are observed. In addition, based on **Figure 16**, different drift values ( $DV$ ) are represented where the different designs and tendons are shown. Here, the  $R_{rel}$  at 25 and 50 cycles are considered since the  $R_{rel}$  below 25 cycles is disturbed by filler-filler and rubber-filler attractions. The sensor with the lowest  $DV$  is recommended as the most stable sensor in the case

of the actuator with an actual  $J(Y)$  of 3 mm by using a SEBS tendon with a  $0.23 \text{ mm}^2$  area. It clarifies the possibility of the proposed CNRC to be used as a hyper-elastic sensor for a tendon-based actuator with a selected composite.

## 5. Conclusions

The processability, electrical conductivity, tensile properties, and piezoresistive behavior of the conductive NR/CNT-CCB composites (CNRC) filled with various mDES loadings were investigated in the presented work. The proper mDES (aZnO:DES) ratio in NR composite of 1:1 was obtained for achieving optimal elastic and electric properties. The combination of appropriate mDES promoted processability well with a shorter cure time and high tensile properties. Additional ionic linkages based on mDES-CNT and mDES-CCB with NR molecules under the proper mDES concentration were the reason behind the enhancement of composite properties. The wettability

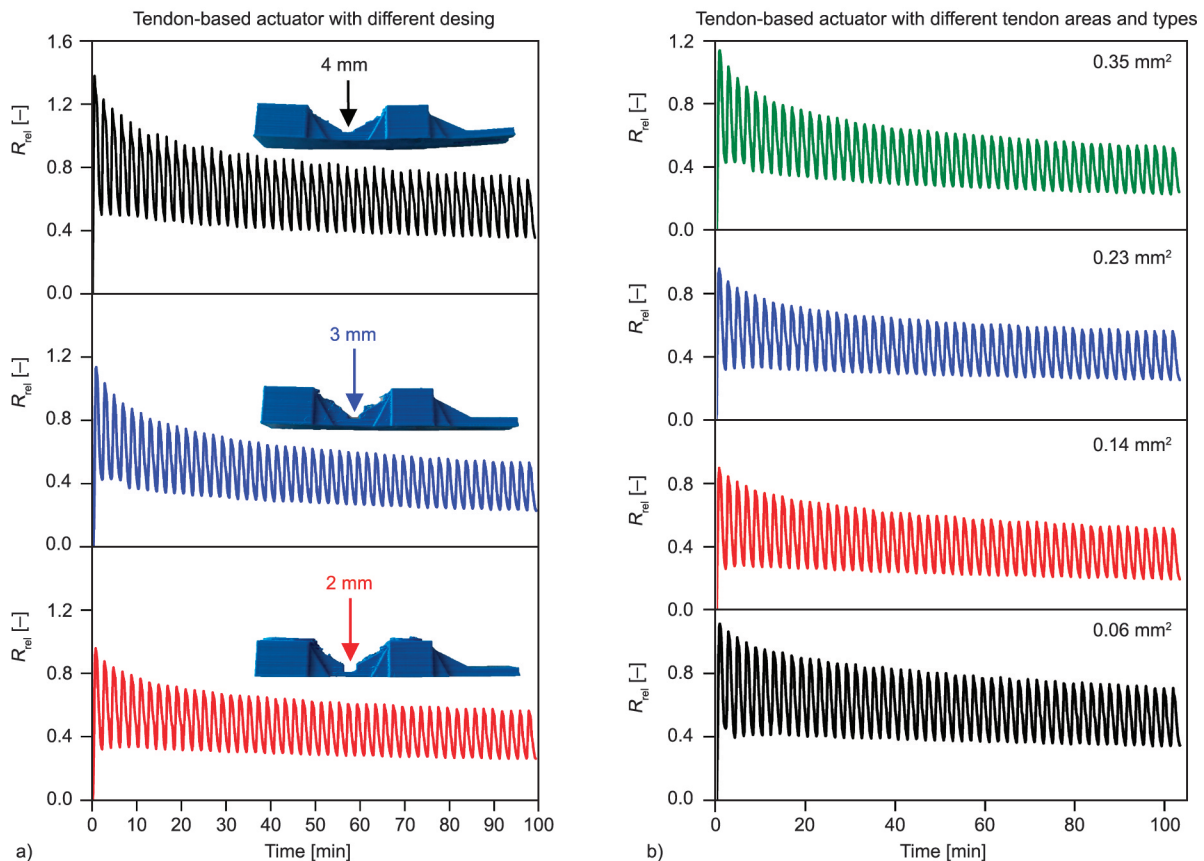


**Figure 16.** Variation in  $R_{rel}$  of CNRC sensor fixed on the actuator during the motion of actuator together with drift value ( $DV$ ) calculated from  $(C_{25} - C_{50}) \cdot 100 / C_{25}$ . Where  $C_{25}$  and  $C_{50}$  refer to  $R_{rel}$  of the composites upon moving for 25 and 50 rounds, respectively. a) Different designs of the actuator by changing the thickness of the hinge at the position of Actual  $J(Y)$  for 2 ( $DV = 13.75$ ), 3 ( $DV = 11.29$ ), and 4 ( $DV = 12.20$ ) mm with the SEBS tendon area of  $0.23 \text{ mm}^2$ . b) Different tendon areas and types of PVC for  $0.06 \text{ mm}^2$  ( $DV = 13.25$ ) and  $0.14 \text{ mm}^2$  ( $DV = 10.86$ ), SEBS for  $0.23 \text{ mm}^2$  ( $DV = 11.63$ ) and PTFE for  $0.35 \text{ mm}^2$  ( $DV = 12.13$ ).

of mDES on the CNT-CCB surfaces provides the opportunity for electron movement even if it was bent from the un-proper relaxation degree of the rubber matrix. This causes CNRC in the presence of mDES to exhibit better sensing response with tunable positive piezoresistivity, while the negative result has occurred in the one without mDES. Under the virtual test of recoverability, reproducibility, and time dependence behavior, the present work demonstrates that the CNRC can be applied in strain sensor applications with balanced sensitivity of proper straining ratio, particularly for the monitoring tendon-based actuator motion. Tunable piezoresistive NR composite was identified as a functional material for newer applications in soft robotics and human body monitoring in the near future.

### Acknowledgements

The authors gratefully acknowledge the financial support from the Post-doctoral Fellowship, King Mongkut's University of Technology Thonburi, and the Thailand Science Research and Innovation (TSRI) under Fundamental Fund 2022 (Project: Advanced Materials and Manufacturing for Applications in new S-curve industries). Also, the funding from the European Union's Horizon 2020 research and the Innovation Program under grant agreement No. 828818 (SHERO Project) and under Marie Skłodowska-Curie grant agreement No. 860108 (SMART PROJECT) are acknowledged.

### References

- [1] Cetin M. S., Toprakci O., Toprakci H. A.: Flexible piezoresistive strain sensors based on carbonaceous filler/thermoplastic elastomer composites. in 'Theory and research in engineering II' (ed.: Kalkanci M.) Gece Publishing, Ankara, Vol. 1, 215–236 (2020).
- [2] Bilotti E., Zhang R., Deng H., Baxendale M., Peijs T.: Fabrication and property prediction of conductive and strain sensing TPU/CNT nanocomposite fibres. *Journal of Materials Chemistry A*, **20**, 9449–9455 (2010).  
<https://doi.org/10.1039/C0JM01827A>
- [3] Zheng Y., Li Y., Dai K., Liu M., Zhou K., Zheng G., Liu C., Shen C.: Conductive thermoplastic polyurethane composites with tunable piezoresistivity by modulating the filler dimensionality for flexible strain sensors. *Composites Part A: Applied Science and Manufacturing*, **101**, 41–49 (2017).  
<https://doi.org/10.1016/j.compositesa.2017.06.003>
- [4] Kumar S., Gupta T., Varadarajan K.: Strong, stretchable and ultrasensitive MWCNT/TPU nanocomposites for piezoresistive strain sensing. *Composites Part B: Engineering*, **177**, 107285 (2019).  
<https://doi.org/10.1016/j.compositesb.2019.107285>
- [5] Sang Z., Ke K., Manas-Zloczower I.: Effect of carbon nanotube morphology on properties in thermoplastic elastomer composites for strain sensors. *Composites Part A: Applied Science and Manufacturing*, **121**, 207–212 (2019).  
<https://doi.org/10.1016/j.compositesa.2019.03.007>
- [6] Melnykowycz M., Koll B., Scharf D., Clemens F.: Comparison of piezoresistive monofilament polymer sensors. *Sensors*, **14**, 1278–1294 (2014).  
<https://doi.org/10.3390/s140101278>
- [7] Georgopoulou A., Sebastian T., Clemens F.: Thermoplastic elastomer composite filaments for strain sensing applications extruded with a fused deposition modelling 3D printer. *Flexible and Printed Electronics*, **5**, 035002 (2020).  
<https://doi.org/10.1088/2058-8585/ab9a22>
- [8] Duan L., Fu S., Deng H., Zhang Q., Wang K., Chen F., Fu Q.: The resistivity-strain behavior of conductive polymer composites: Stability and sensitivity. *Journal of Materials Chemistry A*, **2**, 17085–17098 (2014).  
<https://doi.org/10.1039/C4TA03645J>
- [9] Yang X., Sun L., Zhang C., Huang B., Chu Y., Zhan B.: Modulating the sensing behaviors of poly(styrene-ethylene-butylene-styrene)/carbon nanotubes with low-dimensional fillers for large deformation sensors. *Composites Part B: Engineering*, **160**, 605–614 (2019).  
<https://doi.org/10.1016/j.compositesb.2018.12.119>
- [10] Amjadi M., Pichitpajongkit A., Lee S., Ryu S., Park I.: Highly stretchable and sensitive strain sensor based on silver nanowire-elastomer nanocomposite. *ACS Nano*, **8**, 5154–5163 (2014).  
<https://doi.org/10.1021/nn501204t>
- [11] Zhang B., Li B., Jiang S.: Noncovalently functionalized multi-walled carbon nanotube with core-dualshell nanostructure for improved piezoresistive sensitivity of poly(dimethyl siloxane) nanocomposites. *Composites Part A: Applied Science and Manufacturing*, **94**, 124–132 (2017).  
<https://doi.org/10.1016/j.compositesa.2016.12.008>
- [12] Nakaramontri Y., Kummerlöwe C., Nakason C., Pichaiyut S., Wisunthon S., Clemens F.: Piezoresistive carbon-based composites for sensor applications: Effects of polarity and non-rubber components on shape recovery. *Express Polymer Letters*, **14**, 970–988 (2020).  
<https://doi.org/10.3144/expresspolymlett.2020.79>
- [13] Salaeh S., Das A., Stöckelhuber K. W., Wiessner S.: Fabrication of a strain sensor from a thermoplastic vulcanizate with an embedded interconnected conducting filler network. *Composites Part A: Applied Science and Manufacturing*, **130**, 105763 (2020).  
<https://doi.org/10.1016/j.compositesa.2020.105763>
- [14] Iijima S.: Helical microtubules of graphitic carbon. *Nature*, **345**, 56–58 (1999).  
<https://doi.org/10.1038/354056a0>



- [15] Nakaramontri Y., Nakason C., Kummerlöwe C., Vennemann N.: Influence of modified natural rubber on properties of natural rubber–carbon nanotube composites. *Rubber Chemistry and Technology*, **88**, 199–218 (2015).  
<https://doi.org/10.5254/rct.14.85949>
- [16] Nakaramontri Y., Pichaiyut S., Wisunthorn S., Nakason C.: Hybrid carbon nanotubes and conductive carbon black in natural rubber composites to enhance electrical conductivity by reducing gaps separating carbon nanotube encapsulates. *European Polymer Journal*, **90**, 467–484 (2017).  
<https://doi.org/10.1016/j.eurpolymj.2017.03.029>
- [17] Sumfleth J., Adroher X. C., Schulte K.: Synergistic effects in network formation and electrical properties of hybrid epoxy nanocomposites containing multi-wall carbon nanotubes and carbon black. *Journal of Materials Science*, **44**, 3241–3247 (2009).  
<https://doi.org/10.1007/s10853-009-3434-7>
- [18] Ma P-C., Liu M-Y., Zhang H., Wang S-Q., Wang R., Wang K., Wong Y-K., Tang B-Z., Hong S-H., Paik K-W., Kim J-K.: Enhanced electrical conductivity of nanocomposites containing hybrid fillers of carbon nanotubes and carbon black. *ACS Applied Materials and Interfaces*, **1**, 1090–1096 (2009).  
<https://doi.org/10.1021/am9000503>
- [19] Szeluga U., Kumanek B., Trzebicka B.: Synergy in hybrid polymer/nanocarbon composites. A review. *Composites Part A: Applied Science and Manufacturing*, **73**, 204–231 (2015).  
<https://doi.org/10.1016/j.compositesa.2015.02.021>
- [20] Natarajan T. S., Eshwaran S. B., Stöckelhuber K. W., Wießner S., Pötschke P., Heinrich G., Das A.: Strong strain sensing performance of natural rubber nanocomposites. *ACS Applied Materials and Interfaces*, **95**, 4860–4872 (2017).  
<https://doi.org/10.1021/acsami.6b13074>
- [21] Zhang X. W., Pan Y., Zheng Q., Yi X. S.: Piezoresistance of conductor filled insulator composites. *Polymer International*, **50**, 229–236 (2001).  
[https://doi.org/10.1002/1097-0126\(200102\)50:2<229::AID-PI612>3.0.CO;2-U](https://doi.org/10.1002/1097-0126(200102)50:2<229::AID-PI612>3.0.CO;2-U)
- [22] Das A., Stöckelhuber K. W., Jurk R., Fritzsche J., Klüppel M., Heinrich G.: Coupling activity of ionic liquids between diene elastomers and multi-walled carbon nanotubes. *Carbon*, **47**, 3313–3321 (2009).  
<https://doi.org/10.1016/j.carbon.2009.07.052>
- [23] Subramaniam K., Das A., Stöckelhuber K. W., Heinrich G.: Elastomer composites based on carbon nanotubes and ionic liquid. *Rubber Chemistry and Technology*, **86**, 367–400 (2013).  
<https://doi.org/10.5254/rct.13.86984>
- [24] Maciejewska M., Zaborski M.: Effect of ionic liquids on the dispersion of zinc oxide and silica nanoparticles, vulcanisation behaviour and properties of NBR composites. *Express Polymer Letters*, **8**, 932–940 (2014).  
<https://doi.org/10.3144/expresspolymlett.2014.94>
- [25] Azizi N., Dezfooli S., Hashemi M. M.: A sustainable approach to the Ugi reaction in deep eutectic solvent. *Comptes Rendus Chimie*, **16**, 1098–1102 (2013).  
<https://doi.org/10.1016/j.crci.2013.05.013>
- [26] Sripornsawat B., Thitithammawong A., Tulaphol S., Johns J., Nakaramontri Y.: Positive synergistic effects on vulcanization, mechanical and electrical properties of using deep eutectic solvent in natural rubber vulcanizates. *Polymer Testing*, **96**, 107071 (2021).  
<https://doi.org/10.1016/j.polymertesting.2021.107071>
- [27] Culha U., Nurzaman G., Clemens F., Lida F.: SVAS(3): Strain vector aided sensorization of soft structures. *Sensors*, **14**, 12748–12770 (2014).  
<https://doi.org/10.1088/2058-8585/ab9a22>
- [28] Abbott A. P., Capper G., Davies D. L., Rasheed R. K., Tambyrajah V.: Novel solvent properties of choline chloride/urea mixtures. *Chemical Communications*, **1**, 70–71 (2003).  
<https://doi.org/10.1039/B210714G>
- [29] Guggilla P., Batra A. K., Edwards M. E.: Electrical characterization of LiTaO<sub>3</sub>:P(VDF–TrFE) composites. *Journal of Materials Science*, **44**, 5469–5474 (2009).  
<https://doi.org/10.1007/s10853-009-3753-8>
- [30] Xiang D., Zhang X., Li Y., Harkin-Jones E., Zheng Y., Wang L., Zhao C., Wang P.: Enhanced performance of 3D printed highly elastic strain sensors of carbon nanotube/thermoplastic polyurethane nanocomposites via non-covalent interactions. *Composites Part B: Engineering*, **176**, 107250 (2019).  
<https://doi.org/10.1016/j.compositesb.2019.107250>
- [31] Liu J., Liu Z., Li M., Zhao Y., Shan G., Hu M., Zheng D.: Polydimethylsiloxane nanocomposite filled with 3D carbon nanosheet frameworks for tensile and compressive strain sensors. *Composites Part B: Engineering*, **168**, 175–182 (2019).  
<https://doi.org/10.1016/j.compositesb.2018.12.089>
- [32] Georgopoulou A., Vanderborcht B., Clemens F.: Fabrication of a soft robotic gripper with integrated strain sensing elements using multi-material additive manufacturing. *Frontiers in Robotics and AI*, **8**, 615991 (2021).  
<https://doi.org/10.3389/frobt.2021.615991>
- [33] Georgopoulou A., Michel S., Clemens F.: Sensorized robotic skin based on piezoresistive sensor fiber composites produced with injection molding of liquid silicone. *Polymers*, **13**, 1226 (2021).  
<https://doi.org/10.3390/polym13081226>
- [34] Georgopoulou A., Bosman A. W., Brancart J., Vanderborcht B., Clemens F.: Supramolecular self-healing sensor fiber composites for damage detection in piezoresistive electronic skin for soft robots. *Polymers*, **13**, 2983 (2021).  
<https://doi.org/10.3390/polym13172983>
- [35] Marzec A., Laskowska A., Boiteux G., Zaborski M., Gain O., Serghei A.: The impact of imidazolium ionic liquids on the properties of nitrile rubber composites. *European Polymer Journal*, **53**, 139–146 (2014).  
<https://doi.org/10.1016/j.eurpolymj.2014.01.035>



- [36] Bevilacqua E. M., English E. S.: The scission step in hevea oxidation. *Journal of Polymer Science*, **49**, 495–505 (1961).  
<https://doi.org/10.1002/pol.1961.1204915229>
- [37] Zheng W., Jia Z., Zhang Z., Yang W., Zhang L., Wu S.: Improvements of lanthanum complex on the thermal-oxidative stability of natural rubber. *Journal of Materials Science*, **51**, 9043–9056 (2016).  
<https://doi.org/10.1007/s10853-016-0157-4>
- [38] Nakaramontri Y., Kummerlöwe C., Vennemann N., Wisunthorn S., Pichaiyut S., Nakason C.: Effect of bis(triethoxysilylpropyl) tetrasulfide (TESPT) on properties of carbon nanotubes and conductive carbon black hybrid filler filled natural rubber nanocomposites. *Express Polymer Letters*, **12**, 867–884 (2018).  
<https://doi.org/10.3144/expresspolymlett.2018.75>
- [39] Le H. H., Pham T., Henning S., Klehm J., Wießner S., Stöckelhuber K.-W., Das A., Hoang X. T., Do Q. K., Wu M., Vennemann N., Heinrich G., Radusch H.-J.: Formation and stability of carbon nanotube network in natural rubber: Effect of non-rubber components. *Polymer*, **73**, 111–121 (2015).  
<https://doi.org/10.1016/j.polymer.2015.07.044>
- [40] Chandra A., Bagchi B.: Frequency dependence of ionic conductivity of electrolyte solutions. *The Journal of Chemical Physics*, **112**, 1876–1886 (2000).  
<https://doi.org/10.1063/1.480751>
- [41] Suzuki K., Yataka K., Okumiya Y., Sakakibara S., Sako K., Mimura H., Inoue Y.: Rapid-response, widely stretchable sensor of aligned MWCNT/elastomer composites for human motion detection. *ACS Sensors*, **1**, 817–825 (2016).  
<https://doi.org/10.1021/acssensors.6b00145>
- [42] Duan L., D’Hooge D. R., Cardon L.: Recent progress on flexible and stretchable piezoresistive strain sensors: From design to application. *Progress in Materials Science*, **144**, 100617 (2020).  
<https://doi.org/10.1016/j.pmatsci.2019.100617>
- [43] Sarkawi S. S., Dierkes W. K., Noordermeer J. W. M.: Morphology of silica-reinforced natural rubber: The effect of silane coupling agent. *Rubber Chemistry and Technology*, **88**, 359–372 (2015).  
<https://doi.org/10.5254/rct.15.86936>
- [44] Matchawet S., Nakason C., Kaesaman A.: Electrical and mechanical properties of conductive carbon black filled epoxidized natural rubber. *Advanced Materials Research*, **844**, 255–258 (2014).  
<https://doi.org/10.4028/www.scientific.net/AMR.844.255>
- [45] Matchawet S., Kaesaman A., Vennemann N., Kumerlöwe C., Nakason C.: Effects of imidazolium ionic liquid on cure characteristics, electrical conductivity and other related properties of epoxidized natural rubber vulcanizates. *European Polymer Journal*, **87**, 344–359 (2017).  
<https://doi.org/10.1016/j.eurpolymj.2016.12.037>
- [46] Zhai W., Zhao S., Wang Y., Zheng G., Dai K., Liu C., Shen C.: Segregated conductive polymer composite with synergistically electrical and mechanical properties. *Composites Part A: Applied Science and Manufacturing*, **105**, 68–77 (2018).  
<https://doi.org/10.1016/j.compositesa.2017.11.008>
- [47] Yu S., Wang X., Xiang H., Zhu L., Tebyetekerwa M., Zhu M.: Superior piezoresistive strain sensing behaviors of carbon nanotubes in one-dimensional polymer fiber structure. *Carbon*, **140**, 1–9 (2018).  
<https://doi.org/10.1016/j.carbon.2018.08.028>
- [48] Georgopoulou A., Clemens F.: Piezoresistive elastomer-based composite strain sensors and their applications. *ACS Applied Electronic Material*, **2**, 1826–1842 (2020).  
<https://doi.org/10.1021/acsaem.0c00278>
- [49] Soury H., Banerjee H., Jusufi A., Radacsi N., Stokes A., Park I., Sitti M., Amjadi M.: Wearable and stretchable strain sensors: Materials, sensing mechanisms, and applications. *Advanced Intelligent Systems*, **8**, 2000039 (2020).  
<https://doi.org/10.1002/aisy.202000039>
- [50] Wang Y., Wang Y., Yang Y.: Graphene–polymer nanocomposite-based redox-induced electricity for flexible self-powered strain sensors. *Advanced Energy Materials*, **8**, 1800961 (2018).  
<https://doi.org/10.1002/aenm.201800961>
- [51] Sun J., Kormakov S., Liu Y., Huang Y., Wu D., Yang Z.: Recent progress in metal-based nanoparticles mediated photodynamic therapy. *Molecules*, **23**, 1704–1727 (2018).  
<https://doi.org/10.3390/molecules23071704>
- [52] Shi J., Li X., Cheng H., Liu Z., Zhao L., Yang T., Dai Z., Cheng Z., Shi E., Yang L., Zhang Z., Cao A., Zhu H., Fang Y.: Graphene reinforced carbon nanotube networks for wearable strain sensors. *Advanced Functional Materials*, **26**, 2078–2084 (2016).  
<https://doi.org/10.1002/adfm.201504804>
- [53] Hempel M., Nezich D., Kong J., Hofmann M.: A novel class of strain gauges based on layered percolative films of 2D materials. *Nano Letters*, **12**, 5714–5718 (2012).  
<https://doi.org/10.1021/nl302959a>
- [54] Lin L., Liu S., Zhang Q., Li X., Ji M., Deng H., Fu Q.: Towards tunable sensitivity of electrical property to strain for conductive polymer composites based on thermoplastic elastomer. *ACS Applied Materials and Interfaces*, **5**, 5815–5824 (2013).  
<https://doi.org/10.1021/am401402x>
- [55] Zhou Y., Zhou Y., Deng H., Fu Q.: A novel route towards tunable piezoresistive behavior in conductive polymer composites: Addition of insulating filler with different size and surface characteristics. *Composites Part A: Applied Science and Manufacturing*, **96**, 99–109 (2017).  
<https://doi.org/10.1016/j.compositesa.2017.02.002>

- [56] Zheng Y., Li Y., Dai K., Wang Y., Zheng G., Liu C., Shen C.: A highly stretchable and stable strain sensor based on hybrid carbon nanofillers/polydimethylsiloxane conductive composites for large human motions monitoring. *Composites Science and Technology*, **B**, 276–286 (2018).  
<https://doi.org/10.1016/j.compscitech.2018.01.019>
- [57] Yamaguchi K., Thomas A. G., Busfield J. J. C.: Stress relaxation, creep and set recovery of elastomers. *International Journal of Non-Linear Mechanics*, **68**, 66–70 (2015).  
<https://doi.org/10.1016/j.ijnonlinmec.2014.07.004>
- [58] Wang L., Ding T., Wang P.: Research on stress and electrical resistance of skin-sensing silicone rubber/carbon black nanocomposite during decompressive stress relaxation. *Smart Materials and Structures*, **18**, 065002 (2009).  
<https://doi.org/10.1088/0964-1726/18/6/065002>